

Inferring the effective start dates of non-pharmaceutical interventions during COVID-19 outbreaks

Ilia Kohanovski^a, Uri Obolski^{b,c}, and Yoav Ram^{a,*}

^aSchool of Computer Science, Interdisciplinary Center Herzliya, Herzliya 4610101, Israel

^bSchool of Public Health, Tel Aviv University, Tel Aviv 6997801, Israel

^cPorter School of the Environment and Earth Sciences, Tel Aviv University, Tel Aviv 6997801, Israel

*Corresponding author: yoav@yoavram.com

May 19, 2020

Abstract

During February and March 2020, several countries implemented non-pharmaceutical interventions, such as school closures and lockdowns, with variable schedules to control the COVID-19 pandemic caused by the SARS-CoV-2 virus. Overall, these interventions seem to have successfully reduced the spread of the pandemic. We hypothesize that the official and effective start date of such interventions can significantly differ, for example due to slow diffusion of guidelines in the population, or due to unpreparedness of the authorities and the public. We use an SEIR epidemiological model and an MCMC inference framework to estimate the effective start of NPIs in several countries, and compare this effective dates to the official dates. We report our finding of both late and early effects of NPIs, and discuss potential causes and consequences of our results.

19 Introduction

20 The COVID-19 pandemic has resulted in implementation of extreme non-pharmaceutical interventions
21 (NPIs) in many affected countries. These interventions, from social distancing to lockdowns, are
22 applied in a rapid and widespread fashion. The NPIs are designed and assessed using epidemiological
23 models, which follow the dynamics of the viral infection to forecast the effect of different mitigation and
24 suppression strategies on the levels of infection, hospitalization, and fatality. These epidemiological
25 models usually assume that the effect of NPIs on disease transmission begins at the officially declared
26 date (e.g. Flaxman et al.⁶, Gatto et al.⁸, Li et al.¹¹).

27 Adoption of public health recommendations is often critical for effective response to infectious dis-
28 eases, and has been studied in the context of HIV¹⁰ and vaccination^{4,16}, for example. However,
29 behavioral and social change does not occur immediately, but rather requires time to diffuse in the
30 population through media, social networks, and social interactions. Moreover, compliance to NPIs
31 may differ between different interventions and between people. For example, in a survey of 2,108
32 adults in the UK during Mar 2020, Atchison et al.² found that those over 70 years old were more
33 likely to adopt social distancing than young adults (18-34 years old), and that those with lower income
34 were less likely to be able to work from home and to self-isolate. Similarly, compliance to NPIs may
35 be impacted by personal experiences. Smith et al.¹³ have surveyed 6,149 UK adults in late April
36 and found that people who believe they have already had COVID-19 are more likely to think they are
37 immune, and less likely to comply with social distancing measures. Compliance may also depend on
38 risk perception as perceived by the the number of domestic cases or even by reported cases in other
39 regions and countries. Interestingly, the perceived risk of COVID-19 infection has likely caused a
40 reduction in the number of influenza-like illness cases in the US starting from mid-February¹⁷.

41 Here, we hypothesize that there is a significant difference between the official start of NPIs and their
42 adoption by the public and therefore their effect on transmission dynamics. We use a *Susceptible-*
43 *Exposed-Infected-Recovered* (SEIR) epidemiological model and *Markov Chain Monte Carlo* (MCMC)
44 parameter estimation framework to estimate the effective start date of NPIs from publicly available
45 COVID-19 case data in several geographical regions. We compare these estimates to the official dates
46 and find both late and early effects of NPIs on COVID-19 transmission dynamics. We conclude by
47 demonstrating how differences between the official and effective start of NPIs can confuse assessments
48 of the effectiveness of the NPIs in a simple epidemic control framework.

49 Models and Methods

50 **Data.** We use daily confirmed case data $\mathbf{X} = (X_1, \dots, X_T)$ from several different countries. These
51 incidence data summarize the number of individuals X_t tested positive for SARS-CoV-2 RNA (using
52 RT-qPCR) at each day t . Data for Wuhan, China retrieved from Pei and Shaman¹², data for 11
53 European countries retrieved from Flaxman et al.⁶. Regions in which there were multiple sequences
54 of days with zero confirmed cases (e.g. France), we cropped the data to begin with the last sequence
55 so that our analysis focuses on the first sustained outbreak rather than isolated imported cases. For
56 dates of official NPI dates see Table 1.

57 **SEIR model.** We model SARS-CoV-2 infection dynamics by following the number of susceptible
58 S , exposed E , reported infected I_r , and unreported infected I_u individuals in a population of size N .
59 This model distinguishes between reported and unreported infected individuals: the reported infected
60 are those that have enough symptoms to eventually be tested and thus appear in daily case reports, to
61 which we fit the model.

Country	First	Last
Austria	Mar 10 2020	Mar 16 2020
Belgium	Mar 12 2020	Mar 18 2020
Denmark	Mar 12 2020	Mar 18 2020
France	Mar 13 2020	Mar 17 2020
Germany	Mar 12 2020	Mar 22 2020
Italy	Mar 5 2020	Mar 11 2020
Norway	Mar 12 2020	Mar 24 2020
Spain	Mar 9 2020	Mar 14 2020
Sweden	Mar 12 2020	Mar 18 2020
Switzerland	Mar 13 2020	Mar 20 2020
United Kingdom	Mar 16 2020	Mar 24 2020
Wuhan	Jan 23 2020	Jan 23 2020

Table 1: Official start of non-pharmaceutical interventions. The date of the first intervention is for a ban of public events, or encouragement of social distancing, or for school closures. In all countries except Sweden, the date of the last intervention is for a lockdown. In Sweden, where a lockdown was not ordered during the studied dates, the last date is for school closures. Dates for European countries from Flaxman et al.⁶, date for Wuhan, China from Pei and Shaman¹².

Susceptible (S) individuals become exposed due to contact with reported or unreported infected individuals (I_r or I_u) at a rate β_t or $\mu\beta_t$. The parameter $0 < \mu < 1$ represents the decreased transmission rate from unreported infected individuals, who are often subclinical or even asymptomatic. The transmission rate $\beta_t \geq 0$ may change over time t due to behavioral changes of both susceptible and infected individuals. Exposed individuals, after an average incubation period of Z days, become reported infected with probability α_t or unreported infected with probability $(1 - \alpha_t)$. The reporting rate $0 < \alpha_t < 1$ may also change over time due to changes in human behavior. Infected individuals remain infectious for an average period of D days, after which they either recover, or becomes ill enough to be quarantined. They therefore no longer infect other individuals, and the model does not track their frequency. The model is described by the following equations:

$$\begin{aligned}
\frac{dS}{dt} &= -\beta_t S \frac{I_r}{N} - \mu\beta_t S \frac{I_u}{N} \\
\frac{dE}{dt} &= \beta_t S \frac{I_r}{N} + \mu\beta_t S \frac{I_u}{N} - \frac{E}{Z} \\
\frac{dI_r}{dt} &= \alpha_t \frac{E}{Z} - \frac{I_r}{D} \\
\frac{dI_u}{dt} &= (1 - \alpha_t) \frac{E}{Z} - \frac{I_r}{D}.
\end{aligned} \tag{1}$$

The initial numbers of exposed $E(0)$ and unreported infected $I_u(0)$ are considered model parameters, whereas the initial number of reported infected is assumed to be zero $I_r(0) = 0$, and the number of susceptible is $S(0) = N - E(0) - I_u(0)$. This model is inspired by Li et al.¹¹ and Pei and Shaman¹², who used a similar model with multiple regions and constant transmission β and reporting rate α to infer COVID-19 dynamics in China and the continental US, respectively.

Likelihood function. For a given vector θ of model parameters the *expected* cumulative number of reported infected individuals (I_r) until day t is, following Eq. (1),

$$Y_t(\theta) = \int_0^t \alpha_s \frac{E(s)}{Z} ds, \quad Y_0 = 0. \tag{2}$$

81 We assume that reported infected individuals are confirmed and therefore observed in the daily case
 82 report of day t with probability p_t (note that an individual can only be observed once, and that p_t
 83 may change over time, but t is a specific date rather than the time elapsed since the individual was
 84 infected). We denote by X_t the number of confirmed cases in day t , and by \tilde{X}_t the cumulative number
 85 of confirmed cases until day t ,

$$86 \quad \tilde{X}_t = \sum_{i=1}^t X_i. \quad (3)$$

87 Therefore, at day t the number of reported infected yet-to-be confirmed individuals is $(Y_t(\theta) - \tilde{X}_{t-1})$.
 88 We therefore assume that X_t conditioned on \tilde{X}_{t-1} is Poisson distributed,

$$89 \quad \begin{aligned} (X_1 | \theta) &\sim \text{Poi}(Y_1(\theta) \cdot p_1), \\ (X_t | \tilde{X}_{t-1}, \theta) &\sim \text{Poi}((Y_t(\theta) - \tilde{X}_{t-1}) \cdot p_t), \quad t > 1. \end{aligned} \quad (4)$$

90 Hence, the *likelihood function* $\mathbb{L}(\theta | \mathbf{X})$ for the parameter vector θ given the confirmed case data
 91 $\mathbf{X} = (X_1, \dots, X_T)$ is defined by the probability to observe \mathbf{X} given θ ,

$$92 \quad \mathbb{L}(\theta | \mathbf{X}) = P(\mathbf{X} | \theta) = P(X_1 | \theta) \cdot P(X_2 | \tilde{X}_1, \theta) \cdots P(X_T | \tilde{X}_{T-1}, \theta). \quad (5)$$

93 **NPI model.** To model non-pharmaceutical interventions (NPIs), we set the beginning of the NPIs
 94 to day τ and define

$$95 \quad \beta_t = \begin{cases} \beta, & t < \tau \\ \beta\lambda, & t \geq \tau \end{cases}, \quad \alpha_t = \begin{cases} \alpha_1, & t < \tau \\ \alpha_2, & t \geq \tau \end{cases}, \quad p_t = \begin{cases} 1/9, & t < \tau \\ 1/6, & t \geq \tau \end{cases}, \quad (6)$$

96 where $0 < \lambda < 1$. The values for p_t follow Li et al.¹¹, who estimated the average time between
 97 infection and reporting in Wuhan, China, at 9 days before the start of NPIs and 6 days after start of
 98 NPIs.

99 **Parameter estimation.** To estimate the model parameters from the daily case data \mathbf{X} , we apply a
 100 Bayesian inference approach. We start our model Δt days⁸ before the outbreak (defined as consecutive
 101 days with increasing confirmed cases) in each country. The model in Eq. (1) is parameterized by the
 102 vector θ , where

$$103 \quad \theta = (Z, D, \mu, \{\beta_t\}, \{\alpha_t\}, \{p_t\}, E(0), I_u(0), \tau, \Delta t). \quad (7)$$

104 The likelihood function is defined in Eq. (5). The posterior distribution of the model parameters
 105 $P(\theta | \mathbf{X})$ is estimated using an *affine-invariant ensemble sampler for Markov chain Monte Carlo*
 106 (MCMC)⁹ implemented in the emcee Python package⁷.

107 We defined the following prior distributions on the model parameters $P(\theta)$:

$$\begin{aligned}
Z &\sim \text{Uniform}(2, 5) \\
D &\sim \text{Uniform}(2, 5) \\
\mu &\sim \text{Uniform}(0.2, 1) \\
\beta &\sim \text{Uniform}(0.8, 1.5) \\
\lambda &\sim \text{Uniform}(0, 1) \\
\alpha_1, \alpha_2 &\sim \text{Uniform}(0.02, 1) \\
E(0) &\sim \text{Uniform}(0, 3000) \\
I_u(0) &\sim \text{Uniform}(0, 3000) \\
\tau &\sim \text{TruncatedNormal}\left(\frac{\tau^* + \tau^0}{2}, \frac{\tau^* - \tau^0}{2}, 1, T - 2\right),
\end{aligned} \tag{8}$$

109 where the prior for τ is a truncated normal distribution shaped so that the date of the first and last NPI,
110 τ^0 and τ^* (Table 1), are at minus and plus one standard deviation, and taking values only between
111 1 and $T - 2$, where T is the number of days in the data \mathbf{X} . We have also tested an uninformative
112 uniform prior $U(1, T - 2)$. DIC (see below) was lower for the truncated normal prior in **most coun-**
113 **tries**. More importantly, the uninformative prior could result in non-negligible posterior probability
114 for unreasonable τ values, such as Mar 1 in the United Kingdom. This was probably due to MCMC
115 chains being stuck in low posterior regions of the parameter space. We therefore decided to use the
116 more informative truncated normal prior. Other priors follow Li et al.¹¹, with the following exceptions.
117 λ is used to ensure transmission rates are lower after the start of the NPIs ($\lambda < 1$). We checked values
118 of Δt larger than five days and found they generally produce lower likelihood, higher DIC (see below),
119 and unreasonable parameter estimates, and therefore chose $U(1, 5)$ as the prior.

120 **Model selection.** We perform model selection using DIC (deviance information criterion)¹⁴,

$$\begin{aligned}
DIC(\theta, \mathbf{X}) &= 2\mathbb{E}[D(\theta)] - D(\mathbb{E}[\theta]) \\
&= 2\log \mathcal{L}(\mathbb{E}[\theta] \mid \mathbf{X}) - 4\mathbb{E}[\log \mathcal{L}(\theta \mid \mathbf{X})],
\end{aligned} \tag{9}$$

122 where $D(\theta) = -2\log \mathcal{L}(\theta \mid \mathbf{X})$ is the Bayesian deviance, and expectations $\mathbb{E}[\cdot]$ are taken over the pos-
123 terior distribution $P(\theta \mid \mathbf{X})$. We compare models by reporting their relative DIC; lower is better.

124 **Source code.** We use Python 3 with the NumPy, Matplotlib, SciPy, Pandas, Seaborn, and emcee
125 packages. All source code will be publicly available under a permissive open-source license at
126 github.com/yoavram-lab/EffectiveNPI.

127 Results

128 Several studies have described the effects of non-pharmaceutical interventions in different geographical
129 regions^{6,8,11}. These studies have assumed that the parameters of the epidemiological model change
130 at a specific date, as in Eq. (6), and set the change date τ to the official NPI date τ^* (Table 1). They
131 then fit the model once for time $t < \tau^*$ and once for time $t \geq \tau^*$. For example, Li et al.¹¹ estimate
132 the dynamics in China before and after τ^* at Jan 23. Thereby, they effectively estimate (β, α_1) and
133 (λ, α_2) separately. Here we estimate the posterior distribution $P(\tau \mid \mathbf{X})$ of the *effective* start date of the
134 NPIs by jointly estimating $\tau, \beta, \lambda, \alpha_1, \alpha_2$ on the entire data per region (e.g. Italy, Austria), rather than
135 splitting the data at τ^* . We then estimate the posterior probability $P(\tau \mid \mathbf{X})$ by marginalizing the joint
136 posterior, and estimate $\hat{\tau}$ as the posterior median.

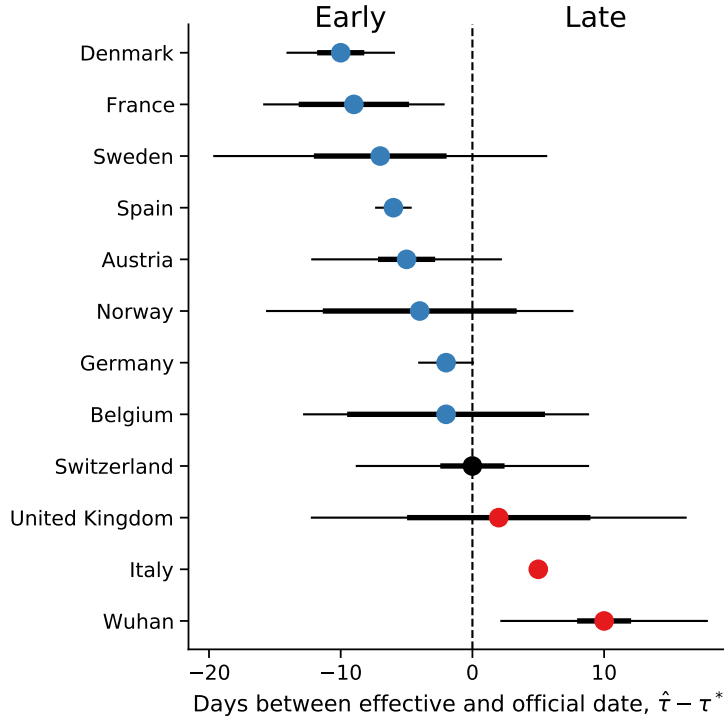


Figure 1: Official and effective start of non-pharmaceutical interventions. The difference between $\hat{\tau}$ the effective and τ^* the official start of NPI is shown for different regions. The effective NPI dates in Italy and Wuhan are significantly delayed compared to the official dates, whereas in Denmark, France, Spain, and Germany, the effective date is earlier than the official date. $\hat{\tau}$ is the posterior median, see Table 2. τ^* is the last NPI date, see Table 1. Thin and bold lines show 95% and 75% credible intervals (area in which $P(|\tau - \hat{\tau}| | \mathbf{X}) = 0.95$ and 0.75.)

137 We find that a model that considers an NPI (Eq. (6)) is a better fit to the data than a model without an
 138 NPI, i.e. with constant β and α ($\Delta DIC > ?$ for all regions.) We compare the official τ^* and effective
 139 $\hat{\tau}$ start of NPIs and find that in some regions the effective start of NPI significantly differs from the
 140 official date (Figure 1): the credible interval on $\hat{\tau}$ does not include τ^* , and the DIC of the model with
 141 free τ parameter is lower than that of a model with a fixed $\tau \equiv \tau^*$ ($\Delta DIC > ?$.)

142 In the following, we describe our findings on late and early effective start of NPI in detail.

143 **Late effective start of NPIs.** In both Wuhan, China, and in Italy we find that our estimated effective
 144 start of NPI $\hat{\tau}$ is significantly later than the official date τ^* (Figure 1).

145 **In Italy**, the first case officially confirmed on Feb 21, a lockdown was declared in Northern Italy on
 146 Mar 8, with social distancing implemented in the rest of the country, and the lockdown was extended
 147 to the entire nation on Mar 11⁸. That is, the official date τ^* is either Mar 8 or 11. However, we
 148 estimate the effective date $\hat{\tau}$ at Mar 16 (± 0.7 days 95% CI ; Figure 2). Similarly, **in Wuhan, China**, a
 149 lockdown was ordered on Jan 23¹¹, but we estimate the effective start of NPIs to be several days later
 150 at around Mar 2 (± 2.65 days 95% CI Figure 2).

151 **Early effective start of NPIs.** In contrast, in some regions we estimate an effective start of NPIs $\hat{\tau}$
 152 that is *earlier* than the official date τ^* (Figure 1). In Spain, social distancing was encouraged starting
 153 on Mar 8⁶, but mass gatherings still occurred on Mar 8, including a march of 120,000 people for the
 154 **International Women's Day**, and a football match between **Real Betis and Real Madrid** (2:1) with a

Country	τ^*	τ	75% CI	95% CI	Z	D	μ	β	α_1	λ	α_2	$E(0)$	$I_u(0)$	Δt
Sweden	Mar 18	Mar 11	5.04	12.68	4.06	3.49	0.43	1.06	0.10	0.62	0.24	261.60	340.99	2.79
Belgium	Mar 18	Mar 16	7.51	10.86	3.96	3.61	0.47	1.10	0.18	0.80	0.36	236.36	307.03	2.66
United Kingdom	Mar 24	Mar 26	6.96	14.27	3.98	3.76	0.64	1.12	0.17	0.71	0.25	144.66	163.83	2.42
Switzerland	Mar 20	Mar 20	2.44	8.86	3.97	3.76	0.62	1.13	0.18	0.47	0.18	107.92	103.17	1.86
Wuhan	Jan 23	Feb 02	2.05	7.88	3.83	3.79	0.64	1.17	0.18	0.20	0.24	331.06	383.46	1.78
Germany	Mar 22	Mar 20	0.54	2.12	3.69	3.97	0.76	1.22	0.28	0.78	0.12	84.89	57.82	1.58
Austria	Mar 16	Mar 11	2.17	7.24	3.97	3.55	0.43	1.10	0.05	0.71	0.47	360.26	399.82	2.59
Spain	Mar 14	Mar 08	0.71	1.39	3.88	3.70	0.60	1.14	0.05	0.73	0.46	637.80	617.46	1.91
France	Mar 17	Mar 08	4.19	6.89	3.96	3.72	0.60	1.14	0.13	0.67	0.36	345.21	364.73	2.14
Italy	Mar 11	Mar 16	0.39	0.51	4.29	3.36	0.49	1.05	0.41	0.44	0.38	313.36	1430.55	1.57
Denmark	Mar 18	Mar 08	1.79	4.12	3.96	3.51	0.39	1.06	0.04	0.31	0.53	339.72	428.69	2.40
Norway	Mar 24	Mar 20	7.36	11.67	4.06	3.40	0.42	1.08	0.13	0.64	0.19	265.91	448.07	2.48

Table 2: Parameter estimates for different regions. See Eq. (1) for model parameters. All estimates are posterior medians. 75% and 95% credible intervals given only for τ , in days. τ^* is the official last NPI date, see Table 1.

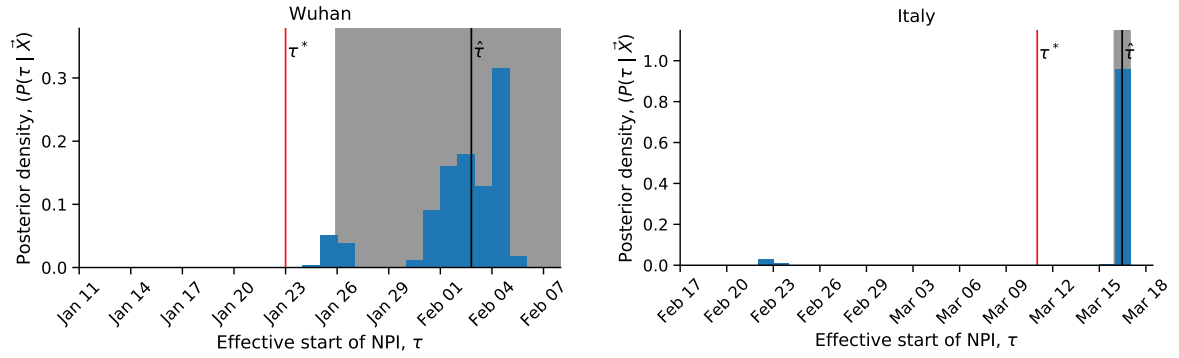


Figure 2: Late effect of non-pharmaceutical interventions in Italy and Wuhan, China. Posterior distribution of τ , the effective start date of NPI, is shown as a histogram of MCMC samples. Red line shows the official last NPI date τ^* . Black line shows the estimated $\hat{\tau}$. Shaded area shows a 95% credible interval (area in which $P(|\tau - \hat{\tau}| | \mathbf{X}) = 0.95$).

crowd of 50,965 in Seville. A national lockdown was only announced on Mar 14⁶. Nevertheless, we estimate the **effective start of NPI** $\hat{\tau}$ at Mar 8 or 9 (± 2.96 95%CI), rather than Mar 14 (Figure 3).

Similarly, in **France** the official lockdown started at Mar 17 (τ^*), with initial NPIs at Mar 13⁶. However, we estimate the effective start of NPIs $\hat{\tau}$ at Mar 8 (± 5.9 days 95% CI). Although the credible interval is wide, spanning from Mar 2 to Mar 13, the official lockdown start at Mar 17 is later still (Figure 3).

Interestingly, the effective start of NPIs $\hat{\tau}$ in both France and Spain is estimated at Mar 8, although the official dates are differ by three days. Moreover, the number of daily cases was similar until Mar 8 in both countries, but diverged by Mar 13, reaching significantly higher numbers in Spain (Figure S2). This may suggest that correlation exist between effective start in NPIs due to global or international events.

The exception that proves the rule. We find one case in which the official and effective dates match: Switzerland ordered a national lockdown on Mar 20, after banning public evens and closing schools on Mar 13 and 14⁶. Indeed, we estimate that $\hat{\tau}$ is **Mar 20**, and the posterior distribution shows two density peaks: a smaller one between Mar 10 and Mar 14, and a taller one between Mar 17 and Mar 22. It's also worth mentioning that Switzerland was the first to mandate self isolation of confirmed cases⁶.

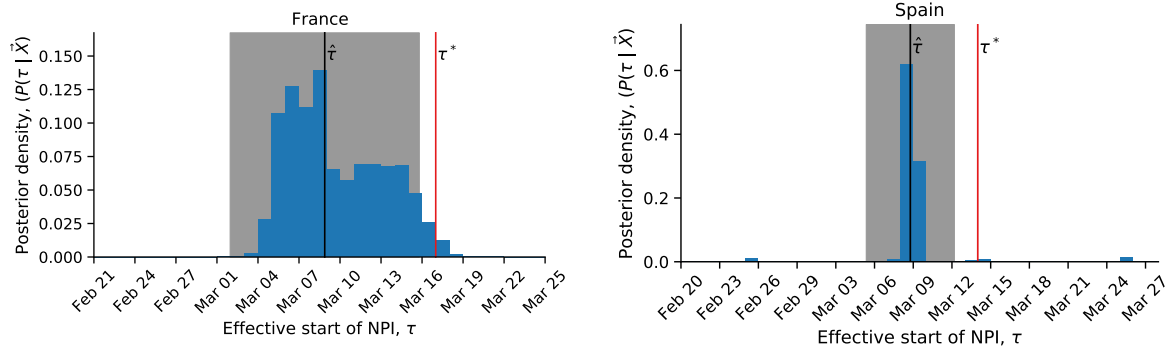


Figure 3: Early effect of non-pharmaceutical interventions in France and Spain. Posterior distribution of τ , the effective start date of NPI, is shown as a histogram of MCMC samples. Red line shows the official last NPI date τ^* . Black line shows the estimated $\hat{\tau}$. Shaded area shows a 95% credible interval (area in which $P(|\tau - \hat{\tau}| | \mathbf{X}) = 0.95$).

Effect of late and early effect of NPIs on real-time assessment. The success of non-pharmaceutical interventions is assessed by health officials using various metrics, such as the decline in the growth rate of daily cases. These assessments are made a specific number of days after the intervention began, to accommodate for the expected serial interval³ (i.e. time between successive cases in a chain of transmission), which is estimated at about 4-7 days⁸.

However, a significant difference between the beginning of the intervention and the effective change in transmission rates can invalidate assessments that assume a serial interval of 4-7 days and neglect the late or early population response to the NPI. Such a case is illustrated in Figure 4 using data and parameters from Italy. Here, a lockdown is officially ordered on Mar 10 (τ^* , but its late effect on the transmission dynamics starts on Mar 15 ($\hat{\tau}$). If health officials assume the dynamics to immediately change at τ^* , they will expect the number of cases to follow the dashed red line. However, the number of cases will actually follow the black line, leading to a significant different (Δ) between the projections and the realization.

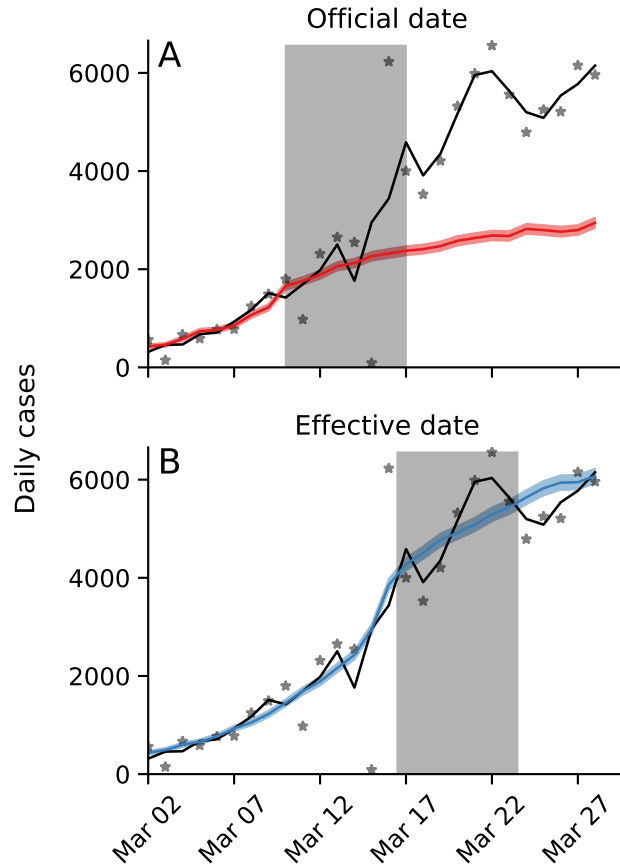


Figure 4: Late effective start of NPIs leads to under-estimation of daily confirmed cases. Real number of daily cases in Italy in black (markers: data, line: time moving average). Model predictions, assuming a 50% decrease in transmission rate after the NPI starts, are shown as colored lines with 95% confidence intervals. Shaded box illustrates a serial interval of seven days. **(A)** Using the official date τ^* for the start of the NPI, the model under-estimates the number of cases seven days after the start of the NPI. **(B)** Using the effective date $\hat{\tau}$ for the start of the NPI, the model correctly estimates the number of cases seven days after the start of the NPI. Here, model parameters are estimates for Italy (Table 2) but with $\lambda = 0.5$ and $\alpha_1 = \alpha_2$.

Discussion

We have estimated the effective start date of NPIs in several geographical regions using an SEIR epidemiological model and an MCMC parameter estimation framework. We find examples of both late and early effect of NPIs (Figure 1).

For example, in Italy and Wuhan, China, the effective start of the lockdowns seems to have occurred 3-5 after the official date (Figure 2). This could be explained by low compliance. In Italy, for example, a leak about the intent to lockdown Northern provinces results in people leaving those provinces⁸. However, late effect of NPIs could also be due to the time required by both the government and the citizens to organize for a lockdown.

In contrast, in most investigated countries, such as Spain and France, transmission rates seem to have been reduced even before official lockdowns were implemented (Figure 3). This early response is possibly due to adoption of social distancing and similar behavioral adaptations in parts of the population, maybe in response increased risk perception due to domestic or international COVID-19-related reports. This finding may also suggest that severe NPIs, such as lockdowns, were unnecessary, and that milder measures that were adopted by the population, possibly due to government recommendations, media coverage, and social networks, could have been sufficient for epidemic control. check if this is

200 **true** Indeed, the evidence supports a change in transmission dynamics (i.e. a model with τ) even for
201 Sweden, in which a lockdown was not implemented, suggesting that lockdowns may not be necessary
202 if other NPIs are adopted early enough during the outbreak³ (Sweden banned public events on Mar 12,
203 encouraged social distancing on Mar 16, and closed schools on Mar 18⁶.)

204 Attempts to assess the effect of NPIs^{3,6} generally assume a 7 day delay between the implementation
205 of the intervention and the observable change in dynamics, due to the characteristic serial interval of
206 COVID-19⁸. However, the late and early effects we have estimated can confuse these assessments and
207 lead to wrong conclusions about the effects of NPIs (Figure 4).

208 We have found that the evidence supports a model in which the parameters change at a specific
209 time point τ over a model without such a change-point. It may be interesting to investigate if the
210 evidence favors a model with *two* change-points, rather than one. Two such change-points could reflect
211 escalating NPIs (e.g. school closures followed by lockdowns), a mix of NPIs and changes in weather,
212 a mix of domestic and international effects on risk perception, or other similar factors.

213 As several countries (e.g. Austria, Israel) begin to relieve lockdowns and ease restrictions, we expect
214 similar delays and advances to occur: in some countries people will begin to behave as if restrictions
215 were eased even before the official date, and in some countries people will continue to self-restrict
216 even after restrictions are officially removed.

217 **Conclusions.** We have estimated the effective start date of NPIs and found that they often differ
218 from the official dates. Our results emphasize the complex interaction between personal, regional,
219 and global determinants of behavioral. Thus, our results highlight the need to further study variability
220 in compliance and behavior over both time and space. This can be accomplished both by surveying
221 differences in compliance within and between populations², and by incorporating specific behavioral
222 models into epidemiological models^{1,5,15}.

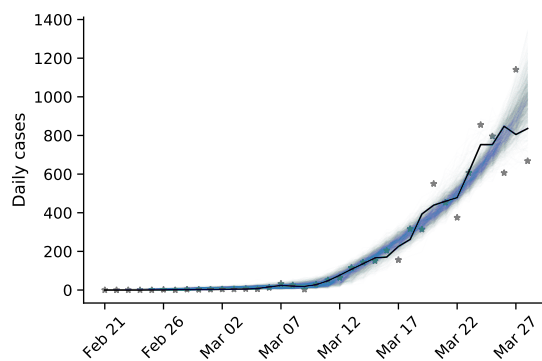
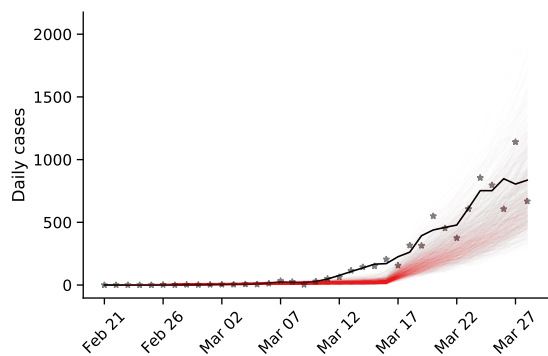
223 **Acknowledgements**

224 This work was supported in part by the Israel Science Foundation 552/19 and 1399/17.

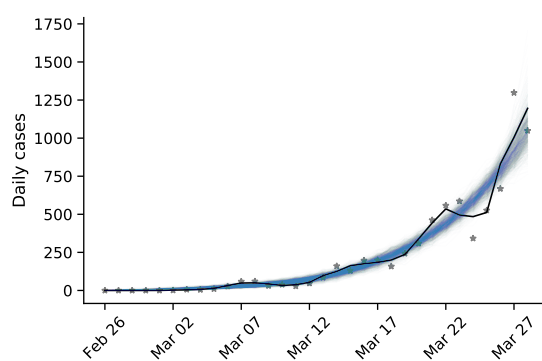
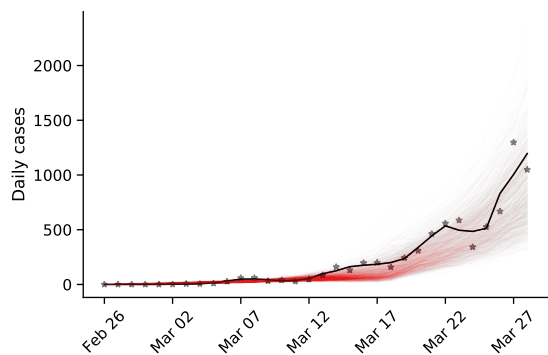
- [1] Arthur, R. F., Jones, J. H., Bonds, M. H. and Feldman, M. W. 2020, 'Complex dynamics induced by delayed adaptive behavior during outbreaks', *bioRxiv* pp. 1–23.
- [2] Atchison, C. J., Bowman, L., Vrinten, C., Redd, R., Pristera, P., Eaton, J. W. and Ward, H. 2020, 'Perceptions and behavioural responses of the general public during the COVID-19 pandemic: A cross-sectional survey of UK Adults', *medRxiv* p. 2020.04.01.20050039.
- [3] Banholzer, N., Weenen, E. V., Kratzwald, B. and Seeliger, A. 2020, 'The estimated impact of non-pharmaceutical interventions on documented cases of COVID-19 : A cross-country analysis', *medRxiv*.
- [4] Dunn, A. G., Leask, J., Zhou, X., Mandl, K. D. and Coiera, E. 2015, 'Associations between exposure to and expression of negative opinions about human papillomavirus vaccines on social media: An observational study', *J. Med. Internet Res.* **17**(6), e144.
- [5] Fenichela, E. P., Castillo-Chavez, C., Ceddiac, M. G., Chowell, G., Gonzalez Parrae, P. A., Hickling, G. J., Holloway, G., Horan, R., Morin, B., Perrings, C., Springborn, M., Velazquez, L. and Villalobos, C. 2011, 'Adaptive human behavior in epidemiological models', *Proc. Natl. Acad. Sci. U. S. A.* **108**(15), 6306–6311.
- [6] Flaxman, S., Mishra, S., Gandy, A., Unwin, J. T., Coupland, H., Mellan, T. A., Zhu, H., Berah, T., Eaton, J. W., Guzman, P. N. P., Schmit, N., Cilloni, L., Ainslie, K. E. C., Baguelin, M., Blake, I., Boonyasiri, A., Boyd, O., Cattarino, L., Ciavarella, C., Cooper, L., Cucunubá, Z., Cuomo-Dannenburg, G., Dighe, A., Djaafara, B., Dorigatti, I., Van Elsland, S., Fitzjohn, R., Fu, H., Gaythorpe, K., Geidelberg, L., Grassly, N., Green, W., Hallett, T., Hamlet, A., Hinsley, W., Jeffrey, B., Jorgensen, D., Knock, E., Laydon, D., Nedjati-Gilani, G., Nouvellet, P., Parag, K., Siveroni, I., Thompson, H., Verity, R., Volz, E., Gt Walker, P., Walters, C., Wang, H., Wang, Y., Watson, O., Xi, X., Winskill, P., Whittaker, C., Ghani, A., Donnelly, C. A., Riley, S., Okell, L. C., Vollmer, M. A. C., Ferguson, N. M. and Bhatt, S. 2020, 'Estimating the number of infections and the impact of non-pharmaceutical interventions on COVID-19 in 11 European countries', *Imp. Coll. London* (March), 1–35.
- [7] Foreman-Mackey, D., Hogg, D. W., Lang, D. and Goodman, J. 2013, 'emcee : The MCMC Hammer', *Publ. Astron. Soc. Pacific* **125**(925), 306–312.
- [8] Gatto, M., Bertuzzo, E., Mari, L., Miccoli, S., Carraro, L., Casagrandi, R. and Rinaldo, A. 2020, 'Spread and dynamics of the COVID-19 epidemic in Italy: Effects of emergency containment measures', *Proc. Natl. Acad. Sci.* p. 202004978.
- [9] Goodman, J. and Weare, J. 2010, 'Ensemble Samplers With Affine Invariance', *Commun. Appl. Math. Comput. Sci.* **5**(1), 65–80.
- [10] Kaufman, M. R., Cornish, F., Zimmerman, R. S. and Johnson, B. T. 2014, 'Health behavior change models for HIV prevention and AIDS care: Practical recommendations for a multi-level approach', *J. Acquir. Immune Defic. Syndr.* **66**(SUPPL.3), 250–258.
- [11] Li, R., Pei, S., Chen, B., Song, Y., Zhang, T., Yang, W. and Shaman, J. 2020, 'Substantial undocumented infection facilitates the rapid dissemination of novel coronavirus (SARS-CoV2)', *Science* (80-.). p. eabb3221.
- [12] Pei, S. and Shaman, J. 2020, 'Initial Simulation of SARS-CoV2 Spread and Intervention Effects in the Continental US', *medRxiv* p. 2020.03.21.20040303.
- [13] Smith, L. E., Mottershaw, A. L., Egan, M., Waller, J., Marteau, T. M. and Rubin, G. J. 2020, 'The impact of believing you have had COVID-19 on behaviour : Cross-sectional survey', *medRxiv* pp. 1–20.
- [14] Spiegelhalter, D. J., Best, N. G., Carlin, B. P. and Van Der Linde, A. 2002, 'Bayesian measures of model complexity and fit', *J. R. Stat. Soc. Ser. B Stat. Methodol.* **64**(4), 583–616.
- [15] Walters, C. E. and Kendal, J. R. 2013, 'An SIS model for cultural trait transmission with conformity bias', *Theor. Popul. Biol.* **90**, 56–63.
- [16] Wiyeh, A. B., Cooper, S., Nnaji, C. A. and Wiysonge, C. S. 2018, 'Vaccine hesitancy – Outbreaks': using epidemiological modeling of the spread of ideas to understand the effects of vaccine related events on vaccine hesitancy', *Expert Rev. Vaccines* **17**(12), 1063–1070.
- [17] Zipfel, C. M. and Bansal, S. 2020, 'Assessing the

interactions between COVID-19 and influenza in the United States', *medRxiv* (February), 1–13.

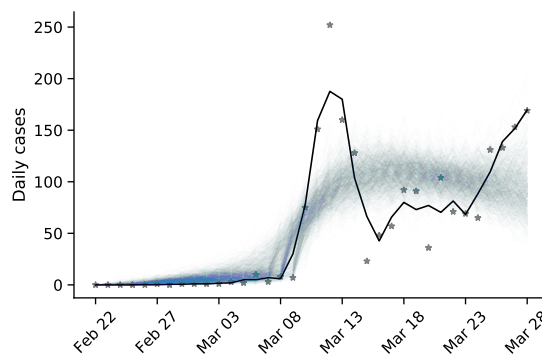
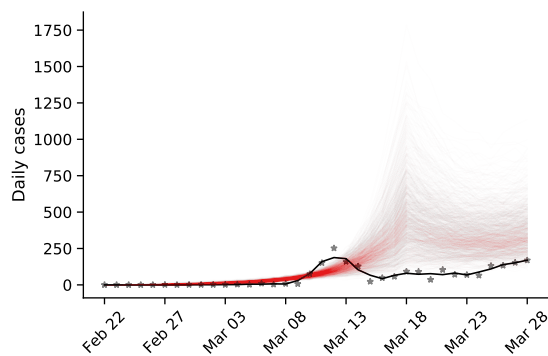
Austria



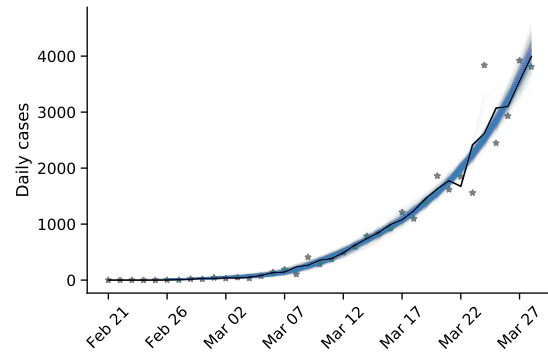
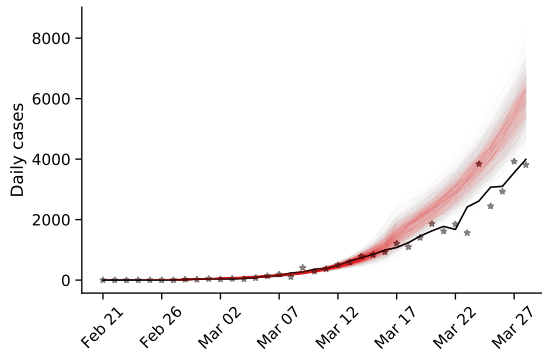
Belgium



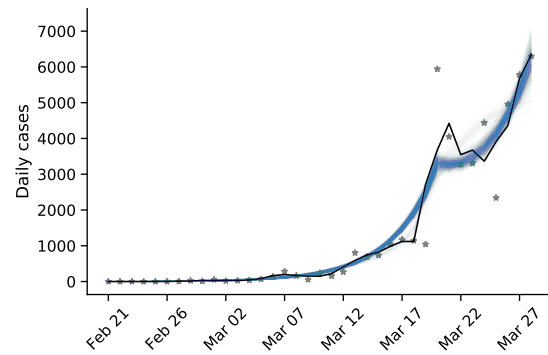
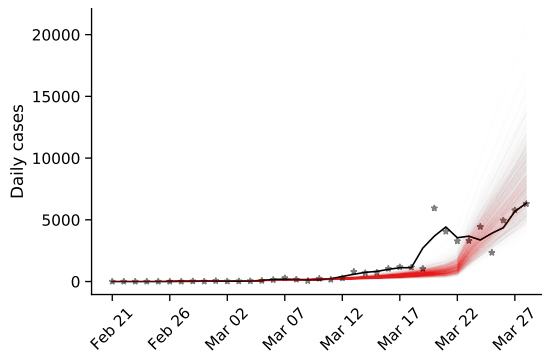
Denmark



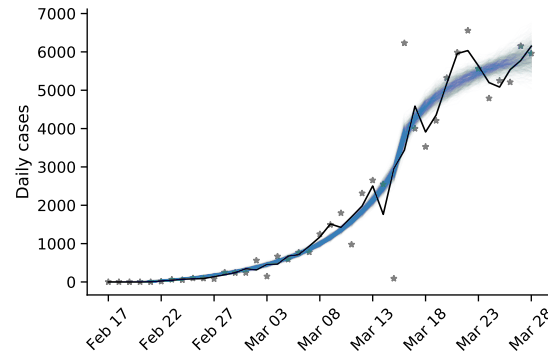
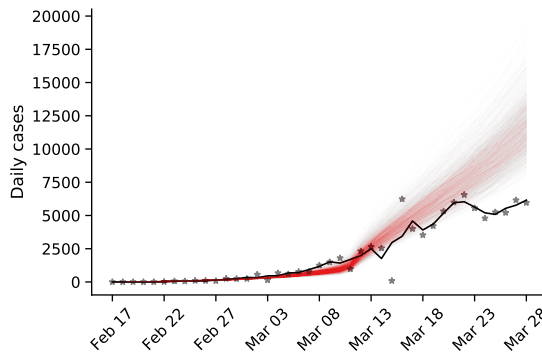
France



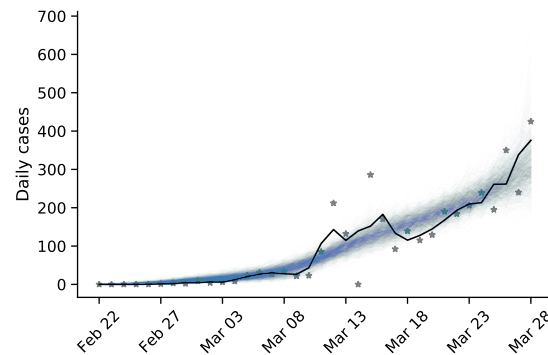
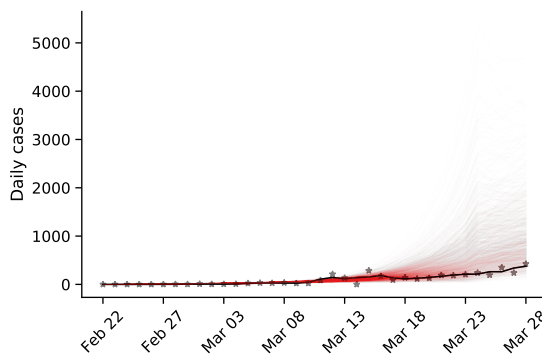
Germany



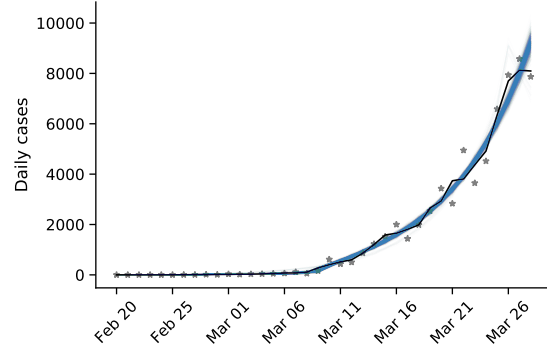
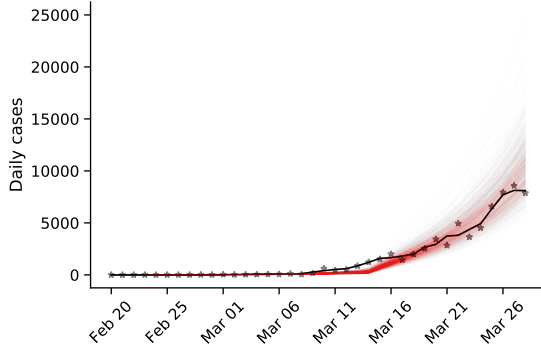
Italy



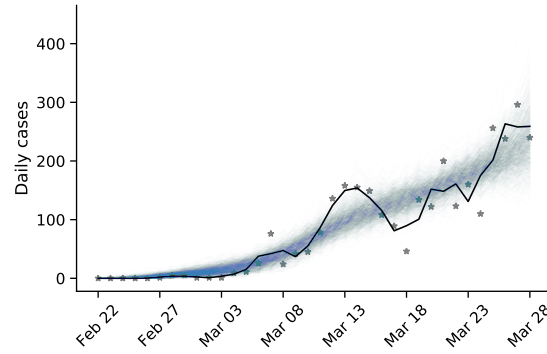
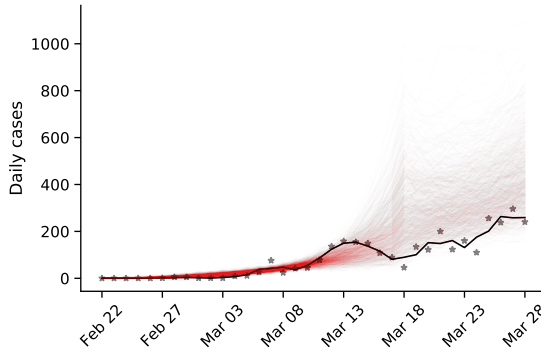
Norway



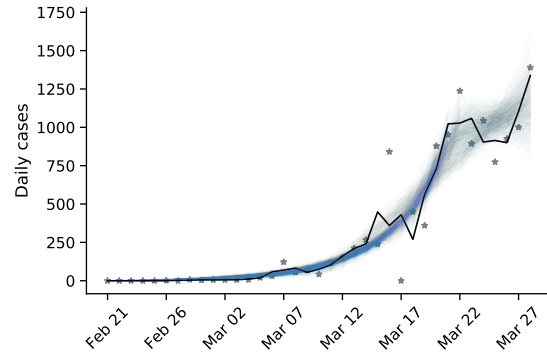
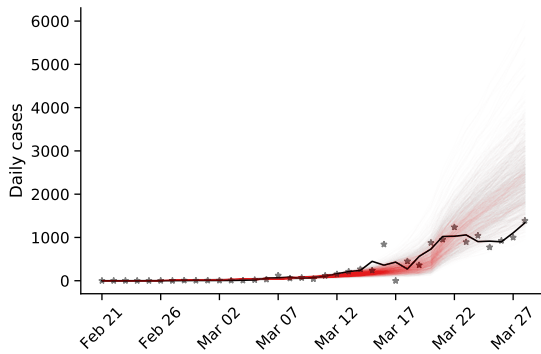
Spain



Sweden



Switzerland



United Kingdom

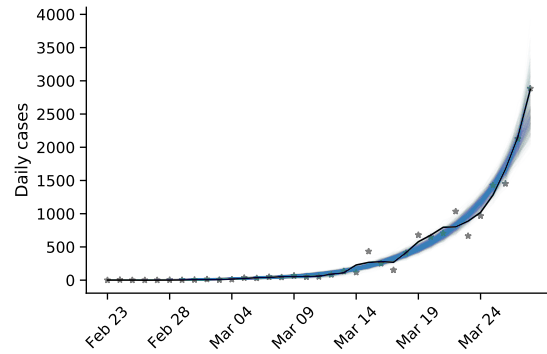
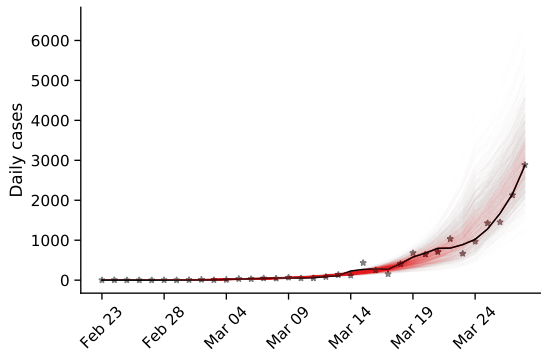


Figure S1. Posterior prediction check plots Markers represent data (X). Black line represent a smoothing of the data points using a Savitzky-Golay filter. Color lines represent posterior predictions from a model with fixed τ , in red, and free τ , in blue. These predictions are made by drawing 1,000 samples from the parameter posterior distribution and then generating a daily case count using the SEIR model in Eq. (1). Note the differences in the y-axis scale.

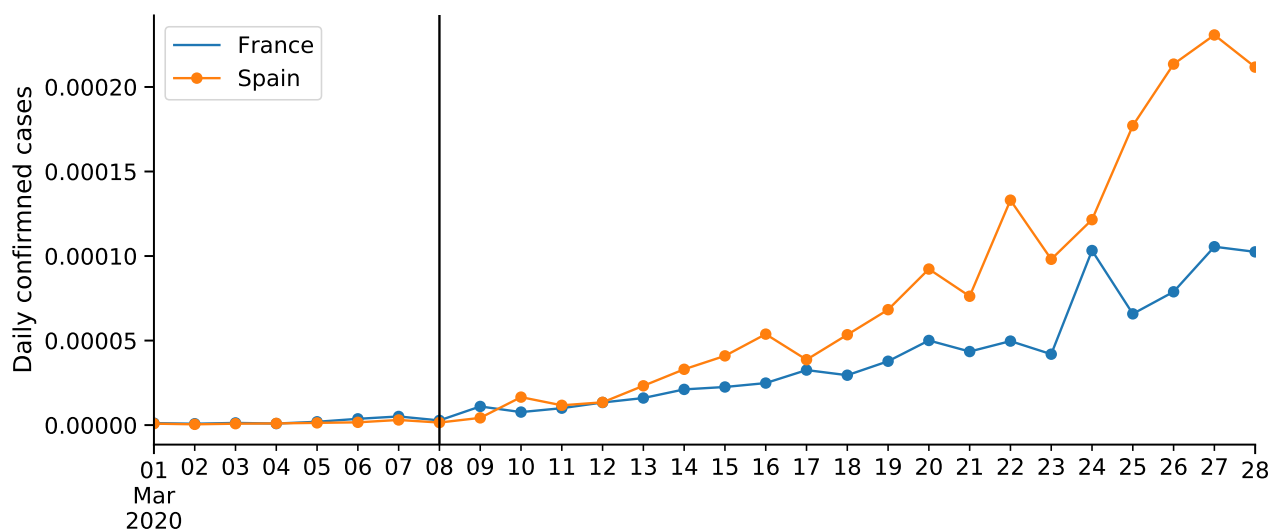


Figure S2: COVID-19 confirmed cases in France and Spain. Number of cases proportional to population size (as of 2018). Vertical line shows Mar 8, the effective start of NPIs $\hat{\tau}$ in both countries.